J. Agr. Sci. Tech. (2012) Vol. 14: 135-147

Introduction to Protein Absorption Lines Index for Relative Assessment of Green Leaves Protein Content Using EO-1 Hyperion Datasets

M. R. Mobasheri[1*], and M. Rahimzadegan[1]

ABSTRACT

The reflectance spectrum of green leaves is considerably affected by their biochemical and biophysical properties. It is possible to extract biochemical information from a continuous vegetation spectrum produced using hyperspectral sensors. The numerous absorption features present in the vegetation spectrum carry a considerable amount of information related to the content and the structure of the leaves and stems. In the present study, we tried to introduce a method for relative quantification of vegetation leaves protein contents using EO-1 Hyperion datasets through an innovative index named *PALI* (Protein Absorption Lines Index). The results of applying *PALI* to *AVIRIS* data also showed its robustness. However, applying *PALI* index for Hyperion images can only show the vegetation leaves protein contents of a pixel relative to its neighboring pixels and not absolute values. Nonetheless, it is assumed that absolute measurements will be possible if one can calibrate this index with field data.

Keywords: Green Leaves, Hyperspectral, Protein, Remote sensing.

INTRODUCTION

The signature of the leaves spectrum is considerably affected by its biochemical and biophysical properties (Card *et al.,* 1988). Hyperspectral technology has made it possible to obtain a continuous spectrum of leaves reflectance from visible to infrared regions of electromagnetic spectrum (ChanSeok *et al.,* 2005). Extraction of leaves biochemical information from a continuous spectrum of reflectance is an important and practically valuable achievement (Darvishzadeh *et al.,* 2007). Green vegetation has unique features around the green (500 to 600 nm), red (600 to 700 nm) and near infrared (700 to 1300 nm) regions of its reflectance spectra (Van der Meer and De Jong, 2001). For example the green peak is due to the chlorophyll which has strong absorption in the red and blue bands (Haboudane *et al.,* 2008; Liang, 2004). On the other hand, leaf tissue causes a large increase in reflectance in the near infrared (NIR) because of cell structure (shape and size) (Alavi Panah *et al.*, 2008). Figure 1 shows typical green leaf absorption features. There are many other absorption features present in the green vegetation spectrum, each one containing a considerable amount of information related to the content and the structure of the leaves and stems. One of the detectable compositions present in green leaves is protein (Lee and Searcy, 2000; Schlerf *et al.,* 2010). Protein is one of the compounds present in leaves that contain Nitrogen (Feng *et al.,* 2008). Protein has nine absorption features centered at 1,020, 1,510, 1,730, 1,980, 2,060, 2,130, 2,180, 2,240 and 2,300 nanometers (Serrano *et al.,* 2002; Liang, 2004). Some of these

[1] Remote Sensing Department, Khaje Nasir Toosi University of Technology, Tehran, Islamic Republic of Iran.
*Corresponding author; e-mail: mobasheri@kntu.ac.ir

[DOR: 20.1001.1.16807073.2012.14.1.18.8]

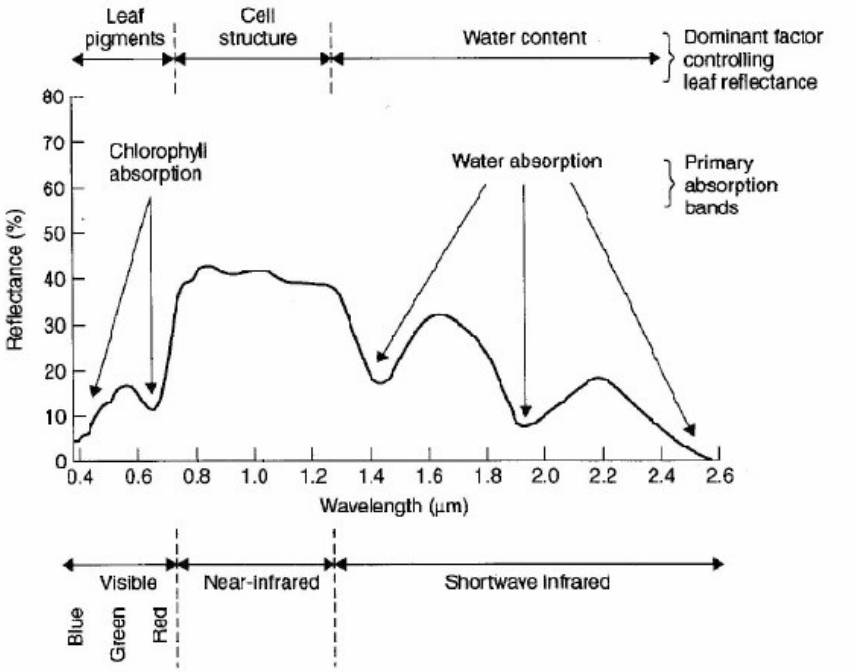

Figure 1. Reflectance spectrum of a sample of green leaf (After Hoffer, 1978).

absorption features are due to the presence of nitrogen whereas some others are related to stretches of O-H and C-H bonds present in the leaf protein compound. Also some of these spectral features are overtones of vibrations in NIR region (Van der Meer and De Jong, 2001). Table 1 shows the reason of the absorption at each of these nine bands (Van der Meer and De Jong, 2001).

Chemical concentrations of vegetation foliage are indicators of the processes conducted by ecosystem (Huanga, *et al.*, 2004). During recent years, remote sensing technology has shown its ability in estimating foliar chemical concentrations over large geographic areas (Curran, 1989). The methodologies have focused on the data collected by spectroradiometers in hundreds of bands in the visible to near-infrared wavelengths, helping identification of chemicals through their many subtle spectral absorption features (Ghasemlu *et al.*, 2010). One of the important foliar chemicals is nitrogen content which is an indicator of photosynthetic rate and overall nutritional status (Curran, 1989) and thus has been the subject of many spectrometric studies details of which can be found in (Huanga *et al.*, 2004). It is worth noting that in such studies the extraction of the reflectance spectra was carried out over entire canopies (Huanga *et al.*, 2004). This is inappropriate for those who are interested in the chemical concentrations of individual leaf or whole trees. As an example, Wallis *et al.* (2002) found that eucalypts show considerable within-species variation in their concentrations of certain chemicals. Of course, many complicating factors have to be considered when one is extending reflectance measurements from dried ground leaves to whole fresh leaves and to entire canopies (Huanga *et al.*, 2004). Indices such as NDVI which is based on the effect of red edge are often used to estimate leaf chlorophyll concentration. This limits the ability of the technique for estimating the concentrations of many other chemicals, such as those containing Nitrogen. This is because Nitrogen has many absorption bands lying outside the red edge region.

[DOR: 20.1001.1.16807073.2012.14.1.18.8]

Table 1. Absorption features related to particular plant compounds (compiled from Elvidge, 1990).

Wavelength (nm)	Absorbing compounds	Absorption mechanism
430	Chlorophyll a	Electron transition
460	Chlorophyll b	Electron transition
640	Chlorophyll b	Electron transition
660	Chlorophyll a	Electron transition
910	Protein	C-H Stretch, 3rd overtone
930	Oil	C-H stretch, 3rd overtone
970	Water, starch	O-H bend, 1st overtone
990	Starch	O-H stretch, 2nd overtone
1020	Protein	N-H stretch
1040	Oil	C-H stretch, C-H deformation
1120	Lignin	C-H stretch, 2nd overtone
1200	Water, cellulose, starch, lignin	O-H bend, 1st overtone
1400	Water	O-H bend, 1st overtone
1420	Lignin	C-H stretch, C-H deformation
1450	Starch, sugar, water, lignin	O-H stretch, 1st overtone, C-H stretch, C-H deformation
1490	Cellulose, sugar	O-H stretch, 1st overtone
1510	Protein, Nitrogen	N-H stretch, 1st overtone
1530	Starch	O-H stretch, 1st overtone
1540	Starch, cellulose	O-H stretch, 1st overtone
1580	Starch, sugar	O-H stretch, 1st overtone
1690	Lignin, starch, protein	C-H stretch, 1st overtone
1730	Protein	C-H stretch
1736	Cellulose	O-H stretch
1780	Cellulose, sugar, starch	C-H stretch, 1st overtone, O-H stretch, H-O-H deformation
1820	Cellulose	O-H stretch, C-O stretch
1900	Starch	O-H stretch, C-O stretch
1924	Cellulose	O-H stretch, O-H deformation
1940	Water, protein, lignin, cellulose, starch, nitrogen	O-H stretch, O-H deformation
1960	Starch, sugar	O-H stretch, O-H rotation
1980	Protein	N-H asymmetry
2000	Starch	O-H deformation, C-O deformation
2060	Protein, nitrogen	N-H stretch, N=H rotation
2080	Starch, sugar	O-H stretch, O-H deformation
2100	Starch, cellulose	O-H rotation, O-H deformation, C-O-C stretch
2130	Protein	N-H stretch
2180	Protein, nitrogen	N-H rotation, C-H stretch, C-O stretch, C=O stretch
2240	Protein	C-H stretch
2250	Starch	O-H stretch, O-H deformation
2270	Cellulose, sugar, starch	C-H stretch, O-H stretch, C-H rotation, CH_2 rotation
2280	Starch, cellulose	C-H stretch, CH_2 deformation
2300	Protein, nitrogen	C-H rotation, C=O stretch, N-H stretch
2310	Oil	C-H bend, 2nd overtone
2320	Starch	C-H stretch, CH_2 deformation
2340	Cellulose	C-H stretch, O-H deformation
2350	Cellulose, nitrogen, protein	CH_2 rotation, C-H deformation

[DOR: 20.1001.1.16807073.2012.14.1.18.8]

Many workers used reflectance spectral derivative for their analysis (Dixit and Ram, 1985; Shah *et al.*, 1990; Tsai and Philpot, 1998; Wessman, 1989). They believe that these derivatives are less sensitive to illumination intensity and background effects and thus can be used for enhancing subtle absorption features of foliar biochemicals. The first and the second derivatives and their approximations are usually combined with different smoothing transformations to estimate foliar chemical concentrations.

In contrast, the Partial Least Squares (PLS) regression method (Wold, 1982) works in a manner similar to principal components analysis. It combines the most useful information from hundreds of bands into the first several factors. The PLS method reduces the effects of canopy background. However it is possible for the nitrogen absorption features to be masked by absorption features of leaf water and leaf chemical contents. To resolve this problem Clark and Roush (1984) suggested using continuum-removal analysis to remove those absorption features of no interest and thus to isolate those individual absorption features of interest (Mutanga *et al.* 2003; Mobasheri *et al.*, 2010).

Kokaly and Clark (1999) were the first to use the continuum-removal analysis method in vegetation studies where they estimated nitrogen, lignin and cellulose concentrations in dried leaves on the ground. The results of Kokaly and Clark (1999) showed that R2 values for nitrogen varied from 0.90 to 0.97 when sample numbers varied from 31 to 193.

Kokaly (2001) further explored that two absorption features centered at 2,054 and 2,172 nm were closely associated with nitrogen concentration. Later on, the methodology was tested by Curran *et al.* (2001) where they compared standard derivative analysis with continuum-removal analysis. They proved that the transformations derived from continuum removal analysis may produce higher R^2 values than what the standard derivative analysis may offer.

In the present study, a method for relative assessment of vegetation leaves protein contents form Hyperion datasets is introduced. However absolute determination of the vegetation leaves protein contents needs field measurements concurrent with the satellite over-passing the area.

Site Selection and Data

The region of study is an agricultural field in the south of Tehran confined between 34.75°N and 35.55°N latitudes and 51.06°E and 51.36°E longitudes (Figure 2). Also Figure 2 shows a map of vegetation cover along with an NDVI image.

In this study a sub-scene of a Hyperion scene is used. The Hyperion sensor is on-board of NASA Earth Observing 1 platform. This sensor has the ability of capturing images in visible-near-infrared (VNIR: 400 to 1300 nm) and shortwave infrared (SWIR: 1,300 to 2,500 nm) regions of spectrum in 224 bands. This enables the sensor to detect and discriminate different features. The spatial resolution of Hyperion is 30 m with a swath width of 7.5 km.

METHODOLOGY

Preprocessing and Atmospheric Correction

From the many types of modules built in ENVI for removing the effects due to the atmospheric interferences from the image, Fast Line-of-sight Atmospheric Analysis of Spectral Hypercubes (FLAASH) was used in this study. This module is based on MODerate resolution TRANSmittance (MODTRAN) algorithm where it needs the image to be primarily converted to physical quantities such as radiance.

The Hyperion image acquired on May 21, 2002 was in Level 1. Only 196 bands out of 224 were calibrated. These bands were 8 to 57 in the visible and near infrared (VNIR) and 77 to 224 for SWIR. One of the problems in Hyperion image is that the sensors VNIR and SWIR have one pixel misplacing after detector 128 in CCD (Charge Coupled Device) array.

[DOR: 20.1001.1.16807073.2012.14.1.18.8]

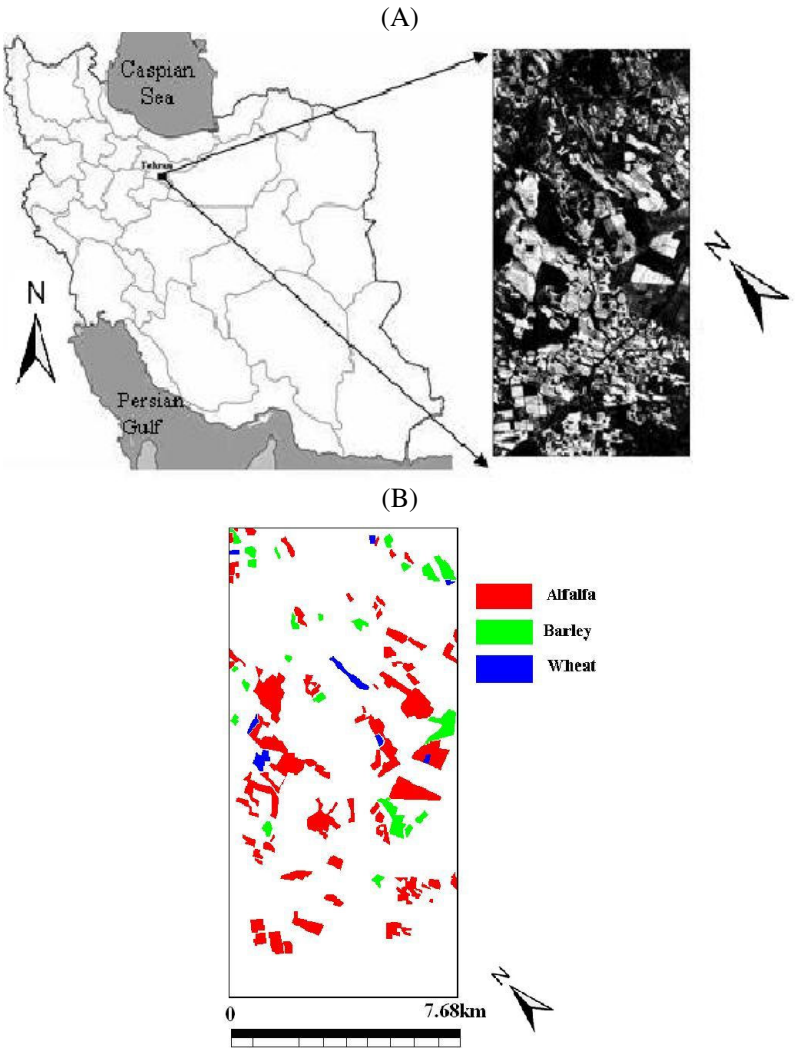

Figure 2. (A): Map of the study area and an NDVI image of the region, (B): Land cover map of different species of vegetation.

This misplacing was corrected where the disappearance of the striping effects was the results of this correction.. Subsequently, the Digital Number (DN) to radiance (*L*) conversion was done using the following equations:

L= Digital number/400, for VNIR region

L= Digital numver/800, for SWIR region (1)

In the next step, by using FLAASH software and entering the horizontal visibility value of 10km reported by the nearest weather station to the study area (code 0III), the relative correction for the atmospheric effects was carried out (Apan *et al.*, 2004; Mobasheri *et al.*, 2007).

Modeling: the *PALI* Index

Our method relies on the fact that the depth of each absorption band is directly proportional to the density of the absorbing materials present in the substances available in each pixel (Serrano *et al.*, 2002). Normally in remote sensing, the Normalized Difference Nitrogen Index (NDNI) is used to detect the

[DOR: 20.1001.1.16807073.2012.14.1.18.8]

$$I_i = \frac{R_{NIR} - R_i}{R_{NIR} + R_i} \quad , \quad i = 1020, 1510, 1730, 1980, 2060, 2130, 2180, 2240, 2300 \qquad (3)$$

vegetation nitrogen content (Serrano *et al.*, 2002). This index is based on the reflectance of two absorbing (1,510 nm) and non-absorbing (1,680 nm) bands which are known as proteins spectral features (Liang, 2004). *NDNI* has the form of:

$$NDNI = \frac{log(1/R_{1510}) - log(1/R_{1680})}{log(1/R_{1510}) + log(1/R_{1680})} \qquad (2)$$

Where R_{1510} and R_{1680} are reflectance values at two absorbing (1,510 nm) and non-absorbing (1,680 nm) bands, respectively. However *NDNI* has some weaknesses one of which being the use of only one absorption band i.e. 1,510 nm. It is likely to have some other substances present in the pixels with high reflectance values at 1,510 nm that could override that of nitrogen absorption band and consequently diminish the absorption feature (Serrano *et al.*, 2002). To overcome this problem, it is suggested to define a new index where more protein absorption bands are deployed. In particular, it is suggested to use one non-absorbing band (highest reflectance) and as many absorption (low reflectance) bands as are present in the protein spectrum. Because the goal of this study was to detect vegetation protein through its nitrogen content, the 1,063.79 nm wavelength seems to be the most suitable non-absorbing band (Feng *et al.*, 2008) along with nine other absorbing bands. Therefore, the suggested indices can be formulated as follows:

where R_{NIR} is reflectance at 1,063.79 nm and R_i is reflectance at *i*th absorbing band (Serrano *et al.*, 2002; Liang, 2004). Using these indices, nine images were produced (Figures 3-a to 3-i). The calculated correlation between each pair of these images was as high as 1.0 and as low as 0.834 (Table 2). This shows that most of the indices produced using Equation (3) are working properly and can be used for protein detection individually. However, as mentioned earlier there might exist some material with higher proportions having high reflectance in some of the protein absorption features causing these features to be hidden causing the relevant index to become very small or even negative. Because the spatial resolution of Hyperion is low (30 m), none of these indices can solely be used for the detection of the small amount of protein in the mixed pixels. An index comprising of all the indices mentioned in Equation (3) may work better particularly for the mixed pixels. On the other hand, since the depths of these absorption bands are different, any emphasis on the stronger absorption bands (if there is any) may result in better detection.

To create this emphasis, the difference between reflectance in NIR and average reflectance in all absorbing bands (bands in wavelengths 1,020, 1,510, 1,730, 1,980, 2,060, 2,130, 2,180, 2,240 and 2,300 nm) are used. Consequently, the following *PALI* index which is a normalization of all absorbing bands is introduced:

$$PALI = \frac{\sum_{i=1}^{n}(R_{NIR} - R_i)}{\sum_{i=1}^{n}(R_{NIR} + R_i)} = \frac{R_{NIR} - \frac{1}{n}\sum_{i=1}^{n} R_i}{R_{NIR} + \frac{1}{n}\sum_{i=1}^{n} R_i} \qquad (4)$$

Where *n* is the number of absorbing bands and the term $\frac{1}{n}\sum_{i=1}^{n} R_i$ in Equation (4) shows the average reflectance in the absorption bands. This may overcome the above-mentioned weakness of *NDNI*. It is found that the range of this index is between 0 and 1.

RESULTS AND DISCUSSION

Because the index suggested in Equation (4) is based on all protein and nitrogen absorbing bands, the higher values of this

[DOR: 20.1001.1.16807073.2012.14.1.18.8]

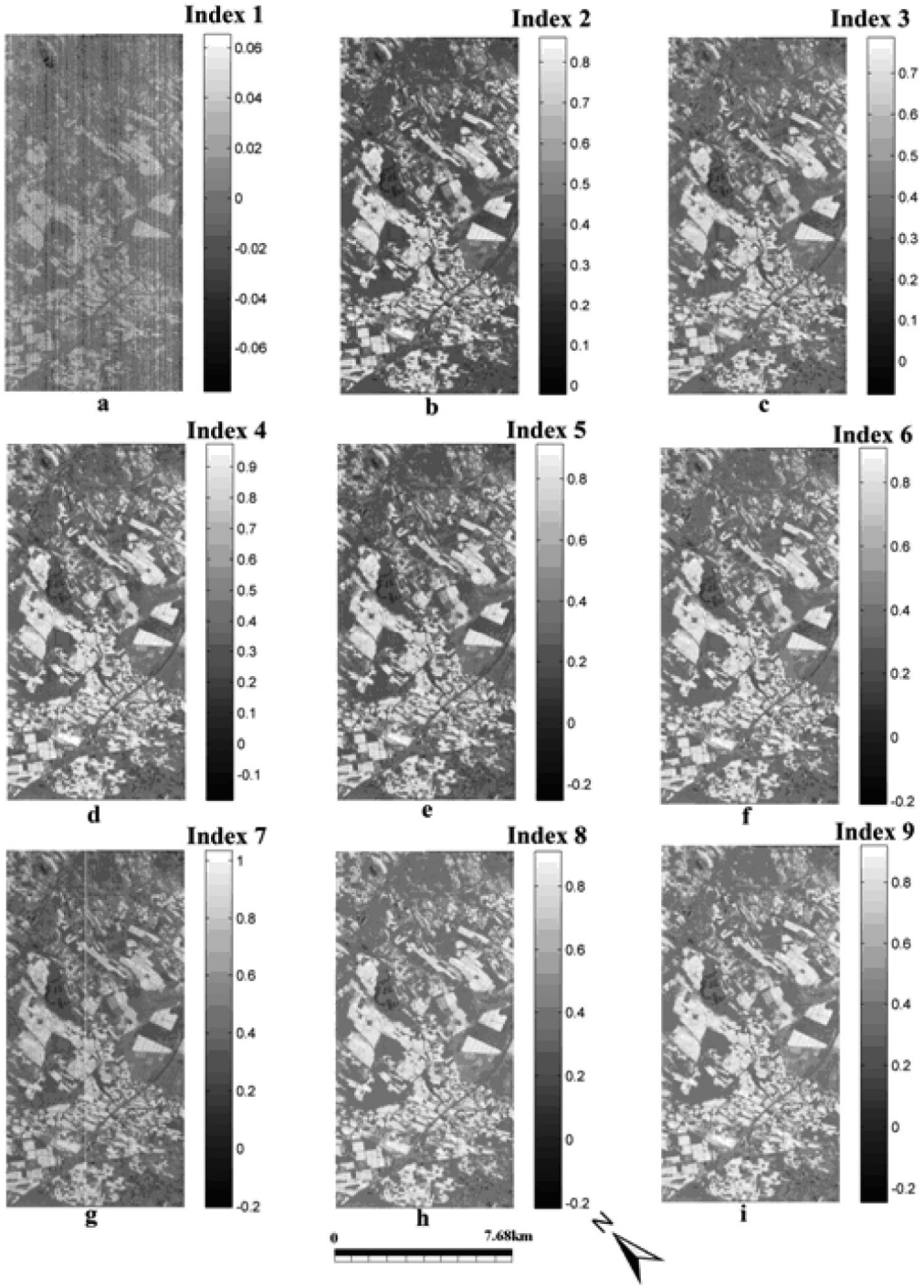

Figure 3. Images of indices produced by applying Equation (3) from left to right (upper) for 1020, 1510, 1730 (middle) 1980, 2060, 2130 and (lower) 2180, 2240, 2300 nm.

[DOR: 20.1001.1.16807073.2012.14.1.18.8]

Table 2. Correlations between each pair of indices presented in Figures 3-a to 3-i.

Index	Figure 3-a	Figure 3b	Figure 3-c	Figure 3-d	Figure 3-e	Figure 3-f	Figure 3-g	Figure 3-h	Figure 3-i
Figure 3-a	1	0.8401	0.8394	0.8369	0.8398	0.837	0.8369	0.8356	0.8341
Figure 3-b	0.8401	1	0.9995	0.9993	0.9979	0.9993	0.9994	0.9991	0.9988
Figure 3-c	0.8394	0.9995	1	0.9988	0.9966	0.9991	0.9995	0.9995	0.9992
Figure 3-d	0.8369	0.9993	0.9988	1	0.9978	0.9992	0.9992	0.9989	0.9987
Figure 3-e	0.8398	0.9979	0.9966	0.9978	1	0.998	0.9971	0.9964	0.9962
Figure 3-f	0.837	0.9993	0.9991	0.9992	0.998	1	0.9994	0.9992	0.9991
Figure 3-g	0.8369	0.9994	0.9995	0.9992	0.9971	0.9994	1	0.9995	0.9994
Figure 3-h	0.8356	0.9991	0.9995	0.9989	0.9964	0.9992	0.9995	1	0.9995
Figure 3-i	0.8341	0.9988	0.9992	0.9987	0.9962	0.9991	0.9994	0.9995	1

index correspond to the pixels containing more protein. Of course there might exist pixels containing vegetation debris in which we might still have high protein contents available while we are not interested in detection of these pixels. In these cases, as a result of R_{NIR} value reduction, the index value drops down to small values and might even take negative values. This is because of the reflectance in NIR band used in the index which is high only for the green vegetation and drops down as the greenness of the vegetation diminishes. Since the goal was the detection of vegetation's protein, only those pixels with $R_{NIR} > R_i$ for all absorption bands are selected. Those pixels not meeting this condition are either water or bare soil or they are not green vegetation so they are set to zero in the output image. Based on the above discussion this index is named *PALI* (Protein Absorption Lines Index). The modeling was done using MATLAB R2008a. The output *PALI* image is shown in Figure 4.

The scatter plot between *PALI* and *NDNI* shows a correlation of about 0.6 (Figure 5). This shows that the two indices are not quite equivalent.

The region A in Figure 5 is the pixels containing boundary regions that should be avoided. This figure shows that both *NDNI* and *PALI* indexes are giving small values for non-vegetated pixels (C in Figure 5). However, for fully vegetated pixels (B), both *NDNI* and PALI give high values. Excluding the A pixels, the correlation coefficient between *PALI* and *NDNI* was about 0.86 with R^2= 0.74 where the number of samples was 129,286. A plot of NDVI and *PALI* is shown in Figure 6. It can be seen in this figure that the NDVI shows

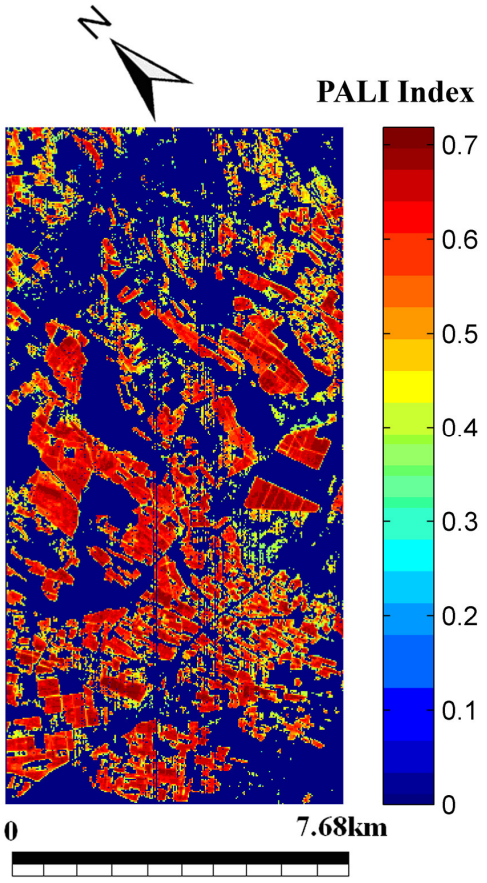

Figure 4. Image of PALI index.

[DOR: 20.1001.1.16807073.2012.14.1.18.8]

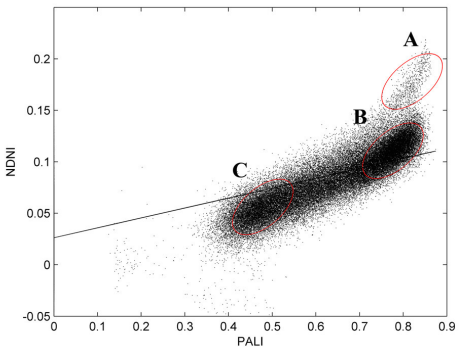

Figure 5. Scatterplot between *NDNI* and *PALI*. The correlation coefficient is found to be 0.86 with R^2= 0.74. Number of samples was 129286.

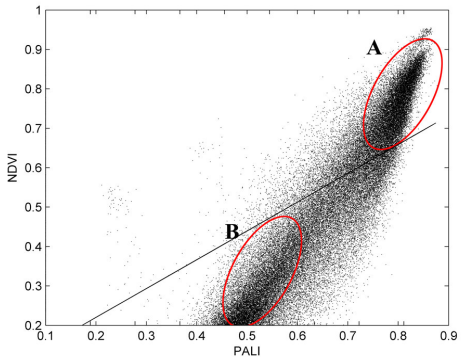

Figure 6. A plot of *NDVI vs. PALI*. The correlation coefficient was 0.93 with R^2= 0.87. Number of samples was 129,286.

values of more than 0.2 (vegetated pixels), and *PALI* varies from 0.5 to 0.9. The scatteredness of points in the region of high NDVI values (A) means that the content of protein in fully vegetated cover pixels might be different from one pixel to the other. This might not be true for low cover pixels (region B in Figure 6) due to mixed pixel effects. The region (A) in Figure 5 has gone into the high NDVI values region in Figure 6 (region A) while it has higher values of NDNI if Figure 5.

Figure 7 is the plot of *NDNI* with respect to NDVI. This figure shows less correlation between fully vegetated pixels (NDVI > 0.5) and *NDNI* compared to the correlation between *PALI* and NDVI in the same region.

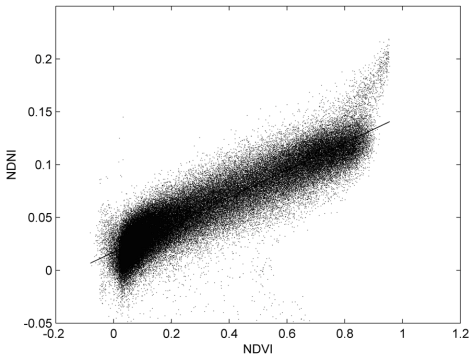

Figure 7. A plot of *NDNI vs.* NDVI. As can be seen the correlation between these two indices is relatively poor.

Comparison between Figures 6 and 7 shows that *PALI* can detect vegetation protein in fully vegetated pixels much better than *NDNI*. This can be due to the sole nitrogen absorption band used in *NDNI* where many non-vegetated pixels (debris) may contain nitrogen and consequently be classified as vegetation protein (Serrano *et al.*, 2002). This cannot happen for the *PALI* because of the deployment of all protein (plus nitrogen) bands in the new index.

To compare calculated *PALI* with those of individual absorption indices of Equation (3), a scatter plot of *PALI* against the mean of nine absorption indices (Mean 9) is shown in Figure 8 where both indices are normalized to one. A correlation coefficient of nearly 1.0 is found between *PALI* and Mean 9 with R^2 of 0.99 where the number of samples was again 129,286.

As can be seen in Figure 8, *PALI* reads lower values compared to Mean 9. This means that some non-vegetated materials may have absorption features in one (or more) of the protein and nitrogen absorption features that may in turn exaggerate the protein content by showing higher values for Mean 9. For low-vegetated and non-vegetated pixels (region A in Figure 8) and boundaries (region B in Figure 8) there was no difference between these two indices.

[DOR: 20.1001.1.16807073.2012.14.1.18.8]

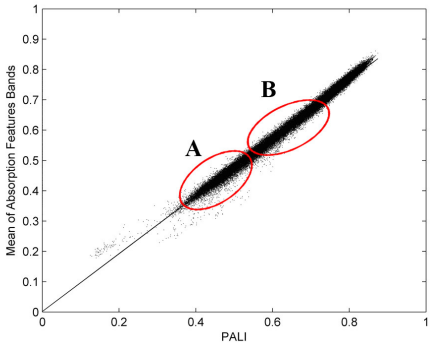

Figure 8. A plot of *PALI* against the mean of nine indices calculated by Equation (3). The correlation coefficient is found to be 1.0 with R^2= 0.99. Number of samples was 129,286.

Method Evaluation

To evaluate the method, *PALI* is applied to an AVIRIS image acquired in June 1992 from an agricultural and forest region located in the north of Indiana State in USA. The AVIRIS is an airborne sensor flying at the altitude of 20 km with spectral resolution of 10nm in 220 bands covering 400 to 2,500 nm spectral region with a spatial resolution of 20m. The available field data is a land cover map containing 16 different classes shown in Figure 9. The color image in Figure 9 is an RGB (17, 27, 50) image. As can be seen in Figure 9, different surface covers including different vegetations are present in the scene and consequently different amounts of protein are expected.

After applying the algorithm to the AVIRIS image, the output classified image is shown in Figure 10. As can be seen in Figure 10, different pixels possess different values of *PALI* equivalent to different amounts of protein in different pixels. Although the precise amount of protein has not been assessed in this field, relative assessment which was the aim and objective of this research has been done successfully. The *PALI* index can assess the absolute magnitude of the protein content if one can calibrate *PALI* by measuring protein content of some samples in the field while the satellite or plane passes over concurrently. In this case the samples will be taken to the laboratory for their precise protein content quantifications where this was not within the scope of this research.

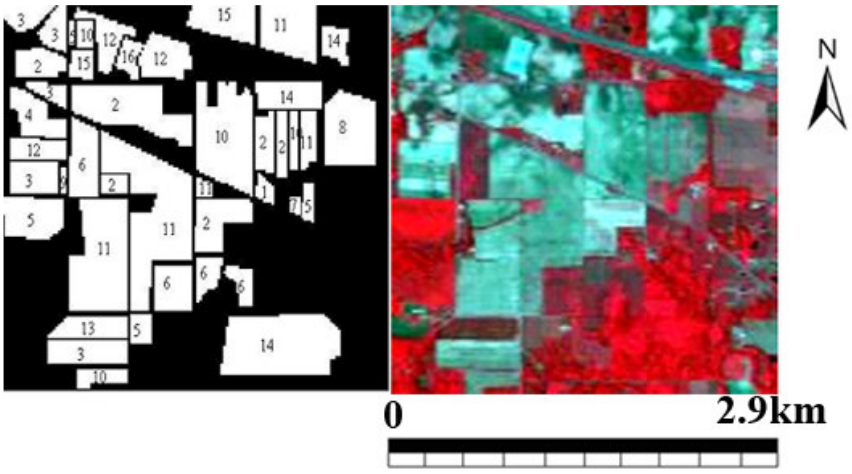

Figure 9. Land cover map (left) and false color image of AVIRIS from the same region (right). The region is an agricultural and forest area located in the north of Indiana State, USA. The classes are: 1: Alfalfa; 2: Corn-notill; 3: Cornmin; 4: Corn; 5: Grass/Pasture; 6: Grass/Trees; 7: Grass/Pasture-mowed; 8: Haywindrowed; 9: Oats; 10: Soy-notill; 11: Soy-min till; 12: Soy-clean; 13: Wheat; 14: Woods; 15: Bldg-grass-trees-drives, 16: Stone-steel towers (Courtesy of [10]).

[DOR: 20.1001.1.16807073.2012.14.1.18.8]

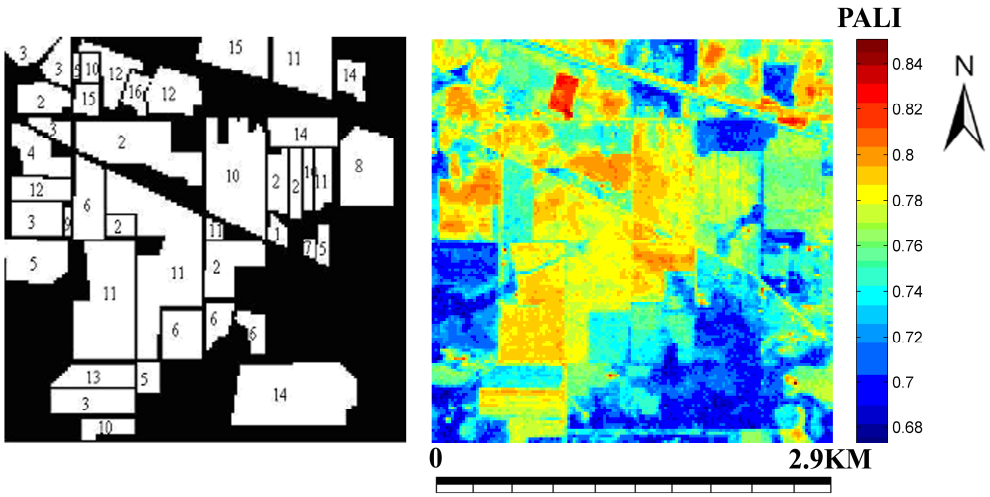

Figure 10. Land cover map (left) and *PALI* index for AVIRIS image (Courtesy of [10]).

CONCLUSIONS

Extraction of biochemical information from a continuous spectrum of reflectance is an important and practically valuable achievement. One of the compositions present in vegetation requiring detection is the vegetation protein content. Protein has nine absorption bands in wavelengths 1,020, 1,510, 1,730, 1,980, 2,060, 2,130, 2,180, 2,240 and 2,300 nanometers. In this work, an index named *PALI* (Protein Absorption Lines Index) for relative quantification of vegetation protein contents is introduced. This index takes all protein absorption bands into account. *PALI* index was applied to Hyperion images as well as AVIRIS where its performance was quite acceptable.

The commonly used index for the nitrogen content is *NDNI*. The *NDNI* index has some weaknesses such as the use of only one absorption band where it is possible to have some other substances present in the pixels with high reflectance values that could override that of protein absorption band and consequently diminish the dip of the absorption feature. This has been overcome in *PALI* index by deploying more protein absorption bands and one non-absorbing band in NIR. The correlation between *PALI* and *NDNI* was poor asserting that *NDNI* may have some difficulties detecting vegetation protein content particularly in the mixed pixels. Of course the correlation between these two indices for fully vegetated pixels was excellent. However the precise amount of protein content has not be assessed in this work but relative assessment which was the aim and objective of this research has been carried out successfully. It is believed that the *PALI* index can be used for assessing the amount of protein content if one can calibrate this index in the field while the satellite or plane passes over concurrently. In this case the samples must be taken to the laboratory for their precise protein content quantifications.

REFERENCES

1. Alavi Panah, S. K., Goossens, R., Matinfar, H. R., Mohamadi, H., Ghadiri, M., Irannegad, H. and Alikhah Asl, M., 2008. The Efficiency of Landsat TM and ETM+ Thermal Data for Extracting Soil Information in Arid Regions. *J. Agr. Sci. Tech*., **10(5):** 439-460.
2. Apan, A., Held, A., Phinn, S. R. and Markley, J. 2004. Detecting Sugarcane 'Orange Rust' Disease Using EO-1 Hyperion

[DOR: 20.1001.1.16807073.2012.14.1.18.8]

Hyperspectral Imagery. *Int. J. Remote Sens.*, **25:** 489-498.

3. Card, D. H., Peterson, D. L., Matson, P. A. and Aber, J. D. 1988. Prediction of Leaf Chemistry by the Use of Visible and Near Infrared Reflectance Spectroscopy. *Remote Sens. Environ.*, **26:** 123-147.
4. ChanSeok, R., Suguri, M., Nishiike, Y. and Umeda, M. 2005. Making Nitrogen Contents Model Using Hyperspectral Remote Sensing and Estimation Nitrogen Content by Nitrogen Content Model. *J. Jap. Soc. Agr.*, **67:** 47-54.
5. Clark, R. N. and Roush, T. L. 1984. Reflectance Spectroscopy: Quantitative Analysis Techniques for Remote Sensing Applications. *J. Geophys. Res.*, **89:** 6329–6340.
6. Curran, P. J. 1989. Remote Sensing of Foliar Chemistry. *Remote Sens. Environ.*, **30:** 271–278.
7. Curran, P. J., Dungan, J. L. and Peterson, D. L. 2001. Estimating the Foliar Biochemical Concentration of Leaves with Reflectance Spectrometry-testing the Kolaly and Clark Methodologies. *Remote Sens. Environ.*, **76**: 349– 359.
8. Darvishzadeh, R., Skidmore, A. K., Schlerf, M., Atzberger, C., Corsi, F. and Cho, M. A. 2008. LAI and Chlorophyll Estimation for a Heterogeneous Grassland Using Hyperspectral Measurements. *ISPRS J. Photogramm. Remote Sens.*, **63:** 409-426.
9. Dixit, L. and Ram, S. 1985. Quantitative Analysis by Derivative Electronic Spectroscopy. *Appl. Spectrosc. Rev.*, **21:** 311 – 418.
10. Elvidge, C. D. 1990. Visible and Near Infrared Reflectance Characteristics of Dry Plant Materials. *Int. J. Remote Sens.*, **11:** 1775-1795.
11. Feng, W., Yao, X., Zhu, Y., Tian, Y. C. and Cao, W. X. 2008. Monitoring Leaf Nitrogen Status with Hyperspectral Reflectance in Wheat. *Eur. J. Agron.*, **28:** 394-404.
12. Ghasemloo, N., Mobasheri, M. R. and Rezaie, Y. 2009. Vegetation Specie Reconnaissance Using Spectral Characteristics and Artificial Neural Network (SCANN). *J. Agr. Sci. Tech.*, (**13**):1223-1232.
13. Haboudane, D., Tremblay, N., Miller, J. R. and Vigneault, P. 2008. Remote Estimation of Crop Chlorophyll Content Using Spectral Indices Derived from Hyperspectral Data. *IEEE Trans. Geosci. Remote Sens.*, **46(2):** 423-437.
14. Huanga, Z., Turnera, B. J., Durya S. J., Wallisb, I. R. and Foley, W. J. 2004. Estimating Foliage Nitrogen Concentration from HYMAP Data Using Continuum Removal Analysis. *Remote Sens. Environ.*, **93:** 18–29.
15. Indiana State, USA 1992. http://dynamo.ecn.purdue.edu/~biehl/multispec/documentation.html
16. Kokaly, R. F. and Clark, R. N. 1999. Spectroscopic Determination of Leaf Biochemistry Using Band-depth Analysis of Absorption Features and Stepwise Multiple Linear Regression. *Remote Sens. Environ.*, **67:** 267– 287.
17. Kokaly, R. F. 2001. Investigating a Physical Basis for Spectroscopic Estimates of Leaf Nitrogen Concentration. *Remote Sens. Environ.*, **75:** 153– 161.
18. Lee, W. S. and Searcy, S. W. 2000. Multispectral Sensor for Detecting Nitrogen in Corn Plants. Paper No. 001010*, Trans. ASAE*, Meeting Paper No. 001010.
19. Liang, S. 2004. *Quantitative Remote Sensing of Land Surfaces*. Wiley and Sons, Hoboken, NJ, USA. PP. 560.
20. Mobasheri, M. R., Rezaei, Y. and Valadan Zoej, M. J. 2007. A Method in Extracting Vegetation Quality Parameters Using Hyperion Images, with Application to Precision Farming. *World Appl. Sci. J.*, **2:** 476-483.
21. Mutanga, O., Skidmore, A. K. and van Wieren, S. 2003. Discriminating Tropical Grass (*Cenchrus ciliaris*) Canopies Grown under Different Nitrogen Treatments Using Spectroradiometry. *ISPRS J. Photogramm. Remote Sens.,* **57:** 263– 272.
22. Schlerf, M., Atzberger, C., Hill, J., Buddenbaum, H., Werner, W. and Schüler, G. 2010. Retrieval of Chlorophyll and Nitrogen in Norway Spruce (*Picea abies* L. Karst.) Using Imaging Spectroscopy. *Int. J. Appl. Earth Obs. Geoinf.*, **12**: 17-26 .
23. Serrano, L., Penuelas, J. and Ustin, S. L. 2002. Remote Sensing of Nitrogen and Lignin in Mediterranean Vegetation from AVIRIS Data: Decomposing Biochemical from Structural Signals. *Remote Sens. Environ.*, **81:** 355-364.
24. Shah, T. H., Steven, M. D. and Clark, J. A. 1990. High Resolution Derivative Spectra in

[DOR: 20.1001.1.16807073.2012.14.1.18.8]

Remote Sensing. *Remote Sens. Environ.*, **33:** 55–64.
25. Tsai, F. and Philpot, W. 1998. Derivative Analysis of Hyperspectral Data. *Remote Sens. Environ.*, **66:** 41– 51.
26. Van der Meer, F. D. and De Jong, S. M. 2001. *Imaging Spectrometry, Basic Principles and Prospective Application*. International Institute for Aerospace survey and Earth Science, ITC, Division of Geological Survey, Kluwer Academic Publishers, Dordrecht, Netherlands, PP. 111-154.
27. Wallis, I. R., Watson, M. L. and Foley, W. J. 2002. Secondary Metabolites in *Eucalyptus melliodora*: Field Distribution and Laboratory Feeding Choices by a Generalist Herbivore, the Common Brushtail Possum. *Aust. J. Zool.*, **50:** 507–519.
28. Wessman, C. A. 1989. Evaluation of Canopy Biochemistry. In: "*Remote Sensing of Biosphere Functioning*", (Eds.): Hobbs, R. J. and Mooney, H. A.. Springer-Verlag, New York, PP. 135– 156.
29. Wold, H. 1982. Soft Modeling, the Basic Design and Some Extensions. Part II. In: "*Systems under Indirect Observation*", (Eds.): Joreskog, K. G. and Wold, H.. North Holland Publishing (Part II), Amsterdam, PP. 1 – 54.

ارائه شاخص *PALI* برای برآورد نسبی محتوای پروتئین برگ سبز گیاهان با استفاده از تصاویر Hyperion

م. ر. مباشری و م. رحیم‌زادگان

چکیده

طیف بازتابندگی گیاهان به‌طور قابل ملاحظه‌ای از خواص بیوشیمیائی و بیوفیزیکی آنها تاثیر می‌پذیرد. این امکان وجود دارد که اطلاعات بیوشیمیائی گیاه را از طیف پیوسته آنها که توسط تصاویر ابرطیفی تولید می‌شود، استخراج نمود. در طیف بازتابندگی گیاهان پدیده‌های جذبی فراوانی وجود دارند که هریک حامل اطلاعات زیادی در رابطه با محتوا و ساختار شاخ و برگ گیاه می‌باشند. در پژوهش حاضر، سعی در معرفی شاخصی جدید به‌نام *PALI* (Protein Absorption Lines Index) برای کمی کردن نسبی میزان پروتئین موجود در گیاهان با استفاده از تصاویر هایپریون شده‌است. نتیجه اعمال شاخص *PALI* بر تصاویر هایپریون و AVIRIS توان و قدرت بالای این شاخص را نشان می‌دهد. به‌هرحال، اعمال شاخص *PALI* بر تصاویر هایپریون تنها می‌تواند محتوای پروتئین برگ گیاهان را به‌طور نسبی و نه به‌طور مطلق در پیکسل‌های مجاور در یک تصویر نشان دهد. البته اعتقاد براین است که می‌توان با اندازه‌گیری‌های میدانی شاخص فوق را به‌گونه‌ای واسنجی نمود که اندازه‌گیری مقادیر واقعی و مطلق پروتئین گیاهان را ممکن سازد.

[DOR: 20.1001.1.16807073.2012.14.1.18.8]